Organizing centres for three-dimensional chemical waves

Arthur T. Winfree

Department of Biological Sciences, Purdue University, West Lafayette, Indiana 47907, USA

Steven H. Strogatz

Division of Applied Sciences, Harvard University, Cambridge, Massachusetts 02138, USA

Excitable media propagate periodic waves of chemical activity. In three dimensions, they resemble scrolls rotating about axes where reactions are not periodic. These axes close in rings which may be linked and knotted, in ways limited by an exclusion principle.

NONLINEAR waves are conspicuous in a variety of biologically and chemically excitable media. Waves of excitation propagate at uniform speed and mutually annihilate in collisions in the Belousov-Zhabotinsky reagent[1-8], in retinal[9] and cortical[10-12] nerve nets, where they may underlie neuromotor pathologies such as epilepsy, in heart muscle[13-16] where they are involved in life-threatening arrhythmias, and in aggregations of social amoebae[17-20] where they coordinate normal development. These waves commonly appear as involute spirals radiating from tiny rotating activity patterns, here called 'organizing centres'. In three-dimensional media, spirals are still seen, now as cross-sections through a scroll-shaped wave[3-5,21-28]. The scroll emanates from its central organizing axis, which typically forms a closed ring. The simplest form of organizing centre is an 'untwisted scroll ring'[1-4,21-28] or 'toroidal vortex'[29]. We present here a chemical/topological exclusion principle that predicts a quantized hierarchy of other, topologically distinct organizing centres and delimits the initial conditions required for their experimental realization[22-28]. We now review the published theoretical, computational, and experimental evidence concerning these three-dimensional reaction-diffusion structures.

Scroll rings

Periodicity is the central principle of all these arrangements of waves. Throughout any region organized by a spiral wave (Fig. 1), each point cycles periodically through activity, refractoriness, quiescence, and activity again. Hence we may describe a snapshot of the pattern in terms of the spatial distribution of phase. The phase, ϕ, of a point means the fraction of a cycle elapsed since the last wavefront excited that point. We represent the phase geometrically as a point on an abstract cycle, the unit circle S^1.

Description of spiral patterns in terms of phase entails a weird topological consequence: there must be a 'phase singularity' in the medium[1-3,23,30]. To prove this, first consider any closed path C enclosing the spiral's inner portions (Fig. 2). In one circuit of C, phase changes through exactly one full cycle. In mathematical terms[1,31], the map $\phi|_C: C \to S^1$ has winding number $W = \pm 1$. To conclude the proof, a theorem of topology[31] asserts that since $W \neq 0$, phase cannot be assigned continuously throughout any disk bounded by C. The most localized discontinuity possible is a phaseless point surrounded by all phases of the cycle: a phase singularity. The immediate neighbourhood of the singularity is a rotating pattern of chemical activities, the pivot of the rotating spiral wave, and the centre from which it radiates.

Because even a thin layer of excitable medium has finite thickness, the ostensibly flat spiral is actually a cross-section of a three-dimensional wave shaped like a scroll. This wave emerges from a filament of singularity. The filament has no physical substance; it cannot be strained out of the liquid like a strand of spaghetti. It represents merely the locus of intersection between two surfaces of uniform chemical concentration[1,3,21-23]. As such, it typically closes in a ring (unless interrupted by the physical boundaries of the medium as in Fig. 2). This predicted exact closure was confirmed experimentally by reconstruction of the fixed wave from serial sections[28,32] and by recent direct video recording during the uninterrupted reaction[4], as well as by computer simulation from the equations of local kinetics and molecular diffusion[3,29]. In the Belousov-Zhabotinsky reagent, these scroll rings persist through about a hundred rotations of the scroll, shrinking slowly at a rate which increases with the curvature of the singular filament[4,21,29,32].

A symmetric caricature of the observed scroll ring is shown in Fig. 3*a*, which depicts a snapshot of the expanding wavefront of excitation. In the next instant, the front would advance a uniform distance at every point and the ring would shrink slightly.

Twists and links

New topologically distinct possibilities exist for scroll ring closure. Imagine forming the ring by bending a straight segment of scroll, then sealing its ends together to preserve continuity (Fig. 3*b*). We might instead have given the straight scroll a 360° twist (Fig. 3*c*), or even have tied knots in it before joining its ends. These structures are indistinguishable locally: in each, a short segment along the singular filament is indistinguishable from a segment of the scroll ring of Fig. 3*a*. Because that untwisted, unknotted scroll ring is viable, local considerations suggest that twisted and knotted rings might be comparably stable.

However, global topology forbids most of these otherwise-plausible organizing centres. Consider, for example, the once-twisted scroll ring (built on the pattern of Fig. 3*c*) that has evolved to fill a cube of the medium. The winding number argument used above to detect a singularity reveals that this solitary once-twisted ring cannot exist: it must be threaded by another singular filament. To prove this, we evaluate the winding number along the inner equator of the invisible torus that confines Fig. 3*b* and *c*. As shown in Fig. 4, W is the number of twists locked into the planar scroll ring. Because $W \neq 0$, any surface bounded by that equator must be punctured by a singular filament[1,24,31].

In a computer-generated image[24,27,28] of the fully evolved wave (Fig. 3*d*), spirals emanate from the singular ring and collide awkwardly along a gnarled helicoidal surface, whose axis is the topologically-inferred phase singularity. This image was constructed by placing an involute spiral in each half-plane extending radially from the ring's axle, and then twisting it through 360° while swinging the plane once about the axle. Gomatam[5] has also shown analytically that such screw

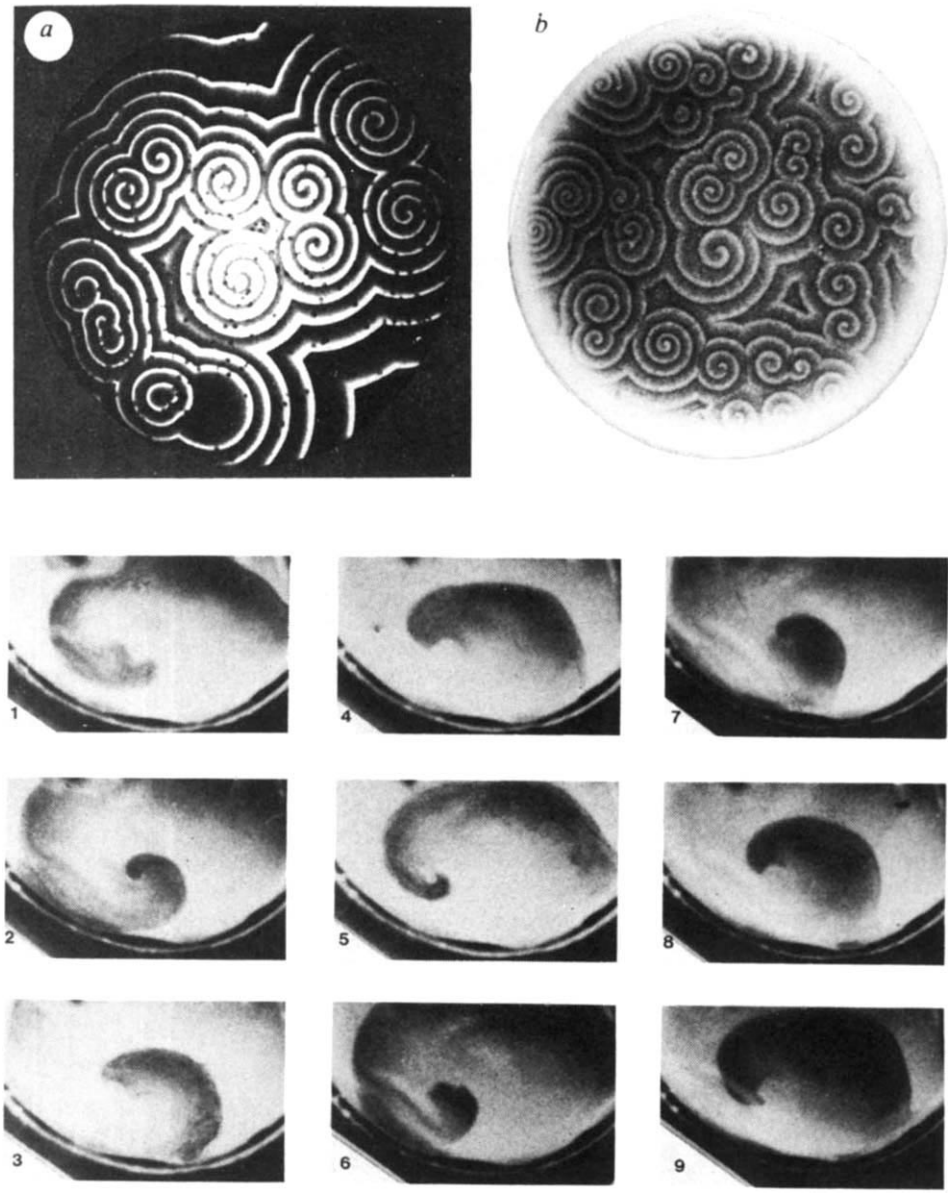

Fig. 1 Rotating spiral waves in excitable media. *a*, Transmitted light photograph of the chemical reagent originated by Belousov[42], and modified[2,7,21]. Waves radiate from spiral centres at a few mm min^{-1}, the spirals turning in about 1 min. The liquid layer is 1 mm deep; the field of view spans 90 mm. *b*, Dark-field photograph of a monolayer of *Dictyostelium discoideum* cells. Cells refract light differently when responding to a pulse of cyclic adenosine monophosphate. The instantaneous loci of this response are spirals rotating once in ~5 min as waves propagate at a few mm min^{-1}. The field of view spans 90 mm (with permission from Newell[20]). *c*, Successive photographs of the retina of a chicken taken by ambient light at intervals of 40 s. The dark area consists of cells recovering behind a wavefront of spreading depression. The front moves ~3 mm min^{-1}, rotating once in 3 min (twice in this mosaic). The field of view is 11 mm × 7.5 mm. (Adapted with permission from Gorelova and Bures[9]).

surface is a solution to linearized reaction–diffusion equations. Because physical rotation is equivalent to time evolution for this particular solution[24], we can animate the intricately rotating, propagating, and self-colliding wavefront by merely spinning it about its vertical axle (ref. 28, and our videotape).

However, there are two reasons why this symmetric solution is best regarded as a limiting extreme of a physically more realistic case. First, observation shows that stable spiral waves in excitable media always radiate outwards from their singularity; here they have been allowed to converge to the axial singularity in Fig. 3*d*. Second, to avoid ending the wave along an unphysical edge, the symmetries of Fig. 3*d* require it to extend to infinity in all directions, in violation of the realistic requirement that waves propagate at finite speed.

The practically realizable (but analytically less convenient) alternative is a pair of identical linked twisted scroll rings. Each provides the necessary threading singularity for the other. Figure 5*a* represents this organizing centre with the horizontal ring viewed nearly edge-on, while the other, regarded as arbitrarily large, is vertical, but hidden behind an interface where waves from each source collide. In Fig. 5*a*, viewports are opened in the horizontal scroll wave as it approaches collision a finite distance from the much larger vertical source ring. Realism is improved in Fig. 5*b* by giving both rings identical radii. Figure 5*b* presents a schematic of comparably sized rings, interlinked by their mutual rotation.

This mated pair of linked scroll rings exists in two mirror-image isomers, each with both singularities left-twisted (as here) or right-twisted. Either can be constructed from toroidal surfaces of uniform chemical concentration[23,24]. Experimental methods to contrive such initial conditions in an excitable medium are suggested elsewhere[23,24]. If its laboratory synthesis is successful the pair of linked twists will be the second observed organizing centre.

Exclusion principle

The allowed anatomy of an organizing centre is quantized by an exclusion principle, derived from both chemical and topological requirements. Away from boundaries of the medium, surfaces of uniform concentration must be disjoint, closed, and orientable; infinite concentration gradients are forbidden; singular filaments must be wave sources, not sinks; and far from the organizing centre, concentrations must approach quiescent uniformity[23]. The exclusion principle then states[26] that any realizable organizing centre must satisfy the constraints that:

$$\sum_{j=1}^{R} L_{ij}N_j = 0 \text{ for each } i = 1, 2, \ldots, R \qquad (1)$$

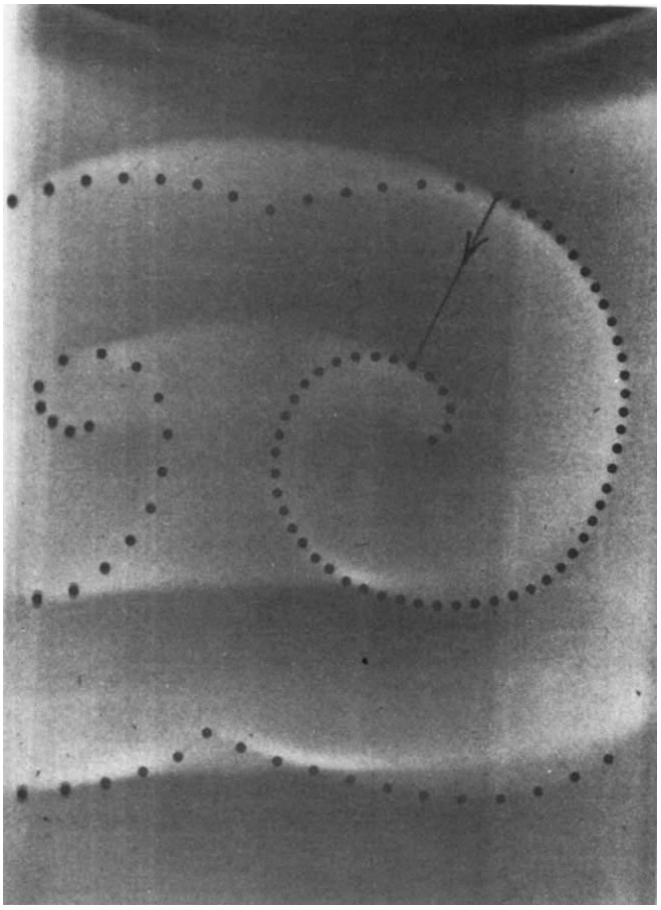

Fig. 2 Untwisted scroll wave and singular filament. A scroll wave in modified[4] Belousov–Zhabotinsky reagent is outlined in dots added to the photograph. Its spiral cross-section is exposed where it encounters the glass wall. A closed curve is traced 360° along this spiral with no change of phase (the chain of closely-spaced dots) then radially through one full wave (the line segment) passing through one full cycle of phase. It is accordingly linked by a singular filament: the scroll's source. (Reproduced with permission from Welsh *et al.*[4].)

where R is the number of constituent rings or knots[25], N_j is the positive number of spiral arms emanating from ring j (the singularity's "topological charge"[6]), L_{ij} is the linking number of rings i and j, and L_{ii} is the linking number of ring i with an imaginary ring traced along the wavefront infinitesimally nearby. These equations dictate the unique integer number L_{ii} of revolutions of the spiral wave required along each ring: $N_i L_{ii}$ must be equal and opposite to the sum of that ring's signed linkages with each of the other rings, counted with multiplicities N_j. L_{ii} is a sum of two real numbers called[25,33,34] the 'twist' (an integral of the spiral's gyration around the ring) and the 'writhing' (which depends only on the shape of the filament itself, and is zero for planar rings).

For a solitary ($R = 1$) ring or knot, the principle requires $L_{ii} = 0$. Thus, it predicts that a solitary scroll ring cannot contain net twist, as proved earlier by winding number arguments, and a solitary scroll knot must be twisted by an amount equal and opposite to its writhing number[25,26,34]. An untwisted ring pair cannot link. A pair of rings may contain equal twists if appropriately linked. For organizing centres composed of more than one ring, equation (1) specifies the set of quantum numbers, N_j, L_{ij}, and L_{ii} compatible with the known constraints. There may be additional constraints forbidding some organizing centres allowed by equation (1).

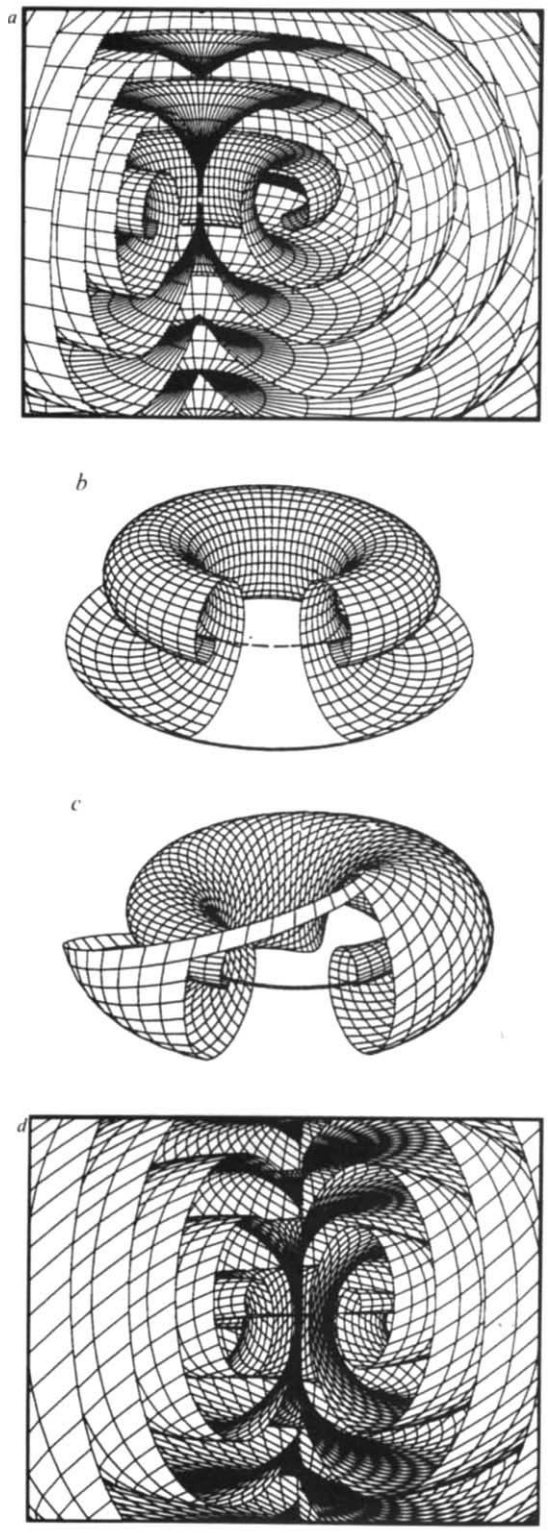

Fig. 3 Computer images of untwisted and twisted scroll rings. *a*, The inner lamina of an untwisted scroll ring wave fill the field of view. Their source is a horizontal circle of phase singularity, the front's inner edge. To aid in visualization, wavefronts are made transparent within a wide sector reaching to the internal symmetry axis along which wavefronts collide. (Reproduced from ref. 28.) *b*, At the same scale, we show as much of *a* as fits inside a torus around the singular ring. The wave's edge is a closed ring. *c*, As in *b* but the contents of the invisible torus are given one full 360° left twist around the circumference. The outer edge of this wave (where it terminates on striking the torus) is still a closed ring, but it now links the torus. *d*, As in *a*, but the wave field is extrapolated from *c* rather than from *b* to fill space. A phase singularity linking the torus is unavoidable. Here it is depicted as the unphysical focus of converging waves. (Reproduced from ref. 28.)

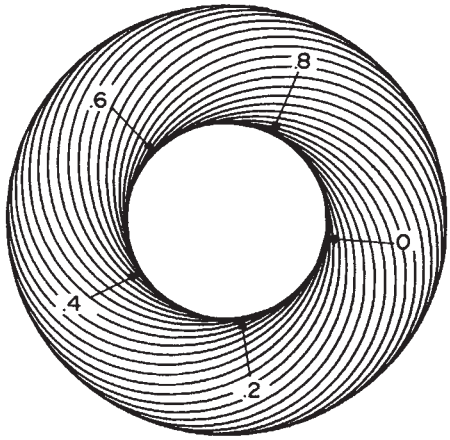

Fig. 4 Successive wavefront positions on a twisted scroll ring. Closed contours of fixed phase on an imaginary toroidal shell enclosing a uniformly once-twisted scroll ring. Only half of each contour is visible. A disk plugging the hole in the toroid touches these phase contours in serial order, spanning one cycle around the disk's boundary. Since $W \neq 0$, the disk must contain a phase singularity[31]. Applying the same argument to every diaphragm bounded by the toroid's inner equator, we detect an unforeseen singular filament threading the twisted scroll ring[1,24].

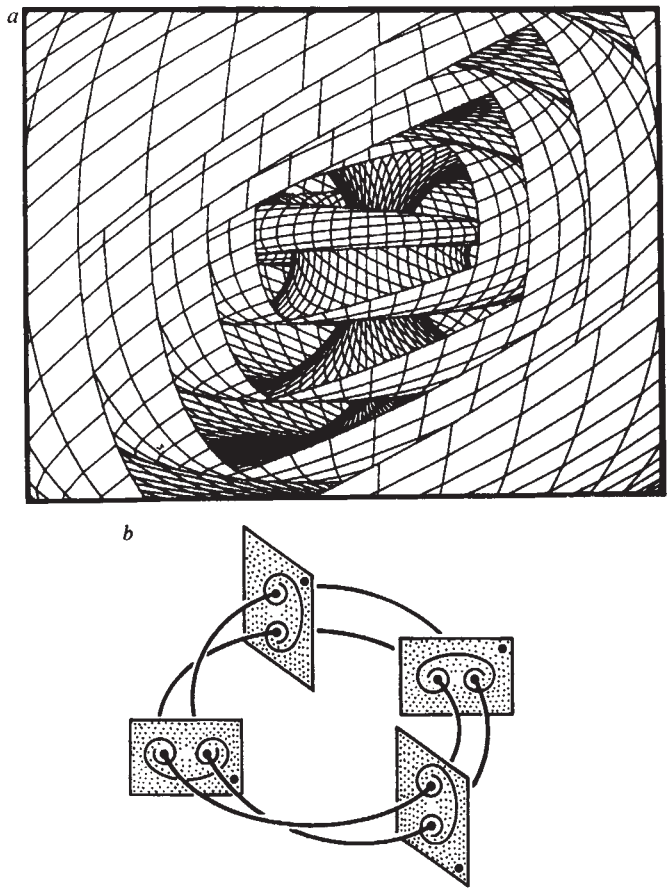

Fig. 5 Mutually linked pair of left-twisted scroll rings. *a*, As in Fig. 3*d*, a once-twisted scroll wave radiates from a horizontal source ring (exposed through a succession of windows). But here the wavefront stops short of collision with itself along an unphysical 'sink'. Rather, it collides with the outgoing wave from the much larger vertical twisted scroll ring hidden in the interior. (Reproduced from ref. 28.) *b*, A mirror-image pair of spirals is transported around a circular path to sweep out a pair of adjacent scrolls. Four local cross-section planes are shown. The pair is rotated as it is transported, so that each scroll is left twisted and the two are mutually linked. Waves emerging from the pair in each cross-section plane eventually join in rings. (Reproduced from ref. 24.)

Transmutation

Solitary scroll rings tend to contract towards their centres of curvature[4,21,29]; it seems likely that the twisted rings of more complex organizing centres do the same. Unless neighbouring filaments repel one another[22], organizing centres in media without boundaries must then eventually decay, leaving behind only quiescent uniformity. (Assuming that there are boundaries, a ring retains the alternative of opening into a scroll wave with an uncurved and stable axis.) Elementary decay processes[3,21] can only involve fission or fusion of rings. It is possible to envision such events in terms of continuous deformation of concentration fields[26]. The result in each case is a rearrangement of quantum numbers which alters R by ± 1 and preserves identities (equation (1)). One allowable transmutation pathway regresses from a solitary trefoil knot to a linked pair of twisted scroll rings to a solitary untwisted scroll ring to an unlinked pair of scroll rings or to spatial homogeneity ('vacuum'). The latter two transmutations have already been observed in a chemically-active medium[37]. Presumably they can also occur in reverse, including the final transmutation to/from the vacuum state. In particular, mechanisms for creating scroll rings *ex nihilo* may have practical importance in biologically excitable media such as heart muscle[38].

Conclusion

We envisage a hierarchy of organizing centres ordered by the number of constituent rings. Loosely analogous to the Periodic Table, this hierarchy contains atoms made of scroll rings, much as in the "vortex atom" notion of Thomson and Helmholtz[39,40]. At each level, diverse isotopes are distinguished by mutual linkage and knotting of rings. Atomic structure is defined by integer quantum numbers, restricted by an exclusion principle. Fission and fusion transmute the elements. However, the geometric periodism peculiar to organizing centres imposes on them a more complex hierarchy than the rows and columns of the Periodic Table.

Attempts are under way to synthesize some of the missing organizing centres, and to observe organizing centres in diverse excitable media. Solitary scroll rings, at least, have been reported in chemically-active media[4,32] and in thick cardiac muscle[38].

Organizing centres could be biologically significant. They emit waves of short period comparable with the absolute minimum attainable, the medium's refractory period. Because waves mutually annihilate in collisions, higher frequency sources eventually dominate slower ones, including normal pacemaker centres, thus usurping control. Although modified by the inhomogeneities of biological media, such organizing centres may be involved with the pathological waves of spreading depression and epilepsy[9–12], and of cardiac fibrillation and sudden death[13–16,38,41].

A.T.W. thanks the NSF for grant CHE-810322, the US Department of Energy and Los Alamos National Laboratory for hospitality and Cray-1 computer time in summer 1983, Mel Prueitt for GRAFIC software and instruction.

1. Winfree, A. T. *The Geometry of Biological Time* (Springer, New York, 1980).
2. Winfree, A. T. *Science* **175**, 634–636 (1972).
3. Winfree, A. T. *Scient. Amer.* **230**(6), 82–95 (1974).
4. Welsh, B., Gomatam, J. & Burgess, A. *Nature* **304**, 611–614 (1983).
5. Gomatam, J. *J. Phys.* **A15**, 1463–1476 (1982).
6. Agladze, K. & Krinsky, V. I. *Nature* **296**, 424–426 (1982).
7. Zaikin, A. N. & Zhabotinsky, A. M. *Nature* **225**, 525–527 (1970).
8. Tyson, J. J. *The Belousov–Zhabotinsky Reaction, Springer Lecture Notes in Biomathematics* Vol. 10 (ed. Levin, S.) (Springer, Berlin, 1976).
9. Gorelova, N. A. & Bures, J. *J. Neurobiol.* **14**, 353–363 (1983).
10. Bures, J., Buresova, O. & Krivanek, J. *The Mechanism and Application of Leao's Spreading Depression of Electroencephalographic Activity* (Academic, Prague, 1974).
11. Koroleva, V. I. & Bures, J. *Brain Res.* **173**, 209–215 (1979).
12. Bures, J., Buresova, O., & Koroleva, V. I. in *Neurophysiological Mechanisms of Epilepsy* (ed. Okujava, V. M.) 120–130 (Metsnierba, Tblisi, 1980).
13. Krinsky, V. I. *Pharm. Ther.* **B3**, 539–555 (1978).
14. Janse, M. J., van Capelle, F. J., Morsink, H. & Kleber, A. G. *Circ. Res.* **47**, 151–165 (1980).
15. Allessie, M. A., Bonke, F. I. M., & Schopman, F. J. G. *Circ. Res.* **333**, 54–62 (1973).
16. van Capelle, F. J. L. & Durrer, D. *Circ. Res.* **47**, 454–466 (1980).
17. Bonner, J. T. *The Cellular Slime Molds* (Princeton University Press, 1967).
18. Gerisch, G. *Current Topics in Developmental Biology* Vol. 3 (eds Moscona, A. & Monroy, A.) 157–197 (Academic, New York, 1968).
19. Tomchik, K. N. & Devreotes, P. N. *Science* **212**, 433–446 (1981).

20. Newell, P. C. in *Fungal Differentiation: a Contemporary Synthesis* (ed. Smith, J.) 43 (Dekker, New York, 1983).
21. Winfree, A. T. *Science* **181**, 937-939 (1973).
22. Winfree, A. T. in *Oscillations and Travelling Waves in Chemical Systems* (eds Field, R. J. & Burger, M.) (Wiley, New York, 1984).
23. Winfree, A. T. & Strogatz, S. H. *Physica* **8D**, 35-49 (1983).
24. Winfree, A. T. & Strogatz, S. H. *Physica* **9D**, 65-80 (1983).
25. Winfree, A. T. & Strogatz, S. H. *Physica* **9D**, 333-345 (1983).
26. Winfree, A. T. & Strogatz, S. H. *Physica* **10D** (in the press).
27. Strogatz, S. H., Prueitt, M. L., & Winfree, A. T. *IEEE Comput. Graphics Appl.* **4**, 66-69 (1984).
28. Winfree, A. T. *Physica* **10D** (in the press).
29. Panfilov, A. & Pertsov, A. M., *Dokl. Akad. Nauk. USSR* **274**, 1500-1503 (1984) (in Russian).
30. Berry, M. V. in *Les Houches Lecture Series* Vol. 35 (eds Bahian, R., Kleman, M., & Poirer, J.-P.) 453-543 (North Holland, Amsterdam, 1981).
31. Munkres, J. R. *Topology: A First Course* 357-360 (Prentice-Hall, Englewood Cliffs, 1975).
32. Winfree, A. T. *Faraday Symp. chem. Soc.* **9**, 38-46 (1974).
33. Crick, F. H. C. *Proc. natn. Acad. Sci.* U.S.A. **73**, 2639-2643 (1976).
34. Fuller, F. B. *Proc. natn. Acad. Sci.* U.S.A. **68**, 815-819 (1971).
35. Pohl, W. F. *Math. Intelligencer* **3**, 20-27 (1980).
36. Bauer, W. R., Crick, F. H. C., & White, J. H. *Scient. Am.* **243**(7), 118-133 (1980).
37. Welsh, B. thesis, Glasgow College of Technology (1984).
38. Medvinsky, A. B., Pertsov, A. M., Polishuk, G. A., & Fast, V. G. in *Electrical Field of the Heart* (eds Baum, O, Roschevsky M. & Titomir, L.) 38-51 (Nauka, Moscow, 1983) (in Russian).
39. Helmholtz, H. *Phil. Mag. Suppl.* **33**, 485-510 (1867).
40. Thomson, W. I. *Phil. Mag.* **34**, 15-24 (1867).
41. Winfree, A. T. *Scient. Am.* **248**(5), 144-161 (1983).
42. Winfree, A. T. *J. chem. Educ.* **61**, 661-663 (1984).

ARTICLES

India–Eurasia collision chronology has implications for crustal shortening and driving mechanism of plates

Philippe Patriat & José Achache

Institut de Physique du Globe de Paris, Université Paris 6, Laboratoire de Géomagnétisme et Paléomagnétisme, 4 Place Jussieu, 75005 Paris, France

The motion of the Indian plate is determined in an absolute frame of reference and compared with the position of the southern margin of Eurasia deduced from palaeomagnetic data in Tibet. The 2,600 ± 900 km of continental crust shortening observed is shown to have occurred in three different episodes: subduction of continental crust, intracontinental thrusting and internal deformation, and lateral extrusion. The detailed chronology of the collision and plate reorganizations in the Indian and Pacific oceans supports the hypothesis that slab-pull is a dominant driving mechanism of plate tectonics.

THE collision between the Indian and Eurasian continents is considered to be one of the major tectonic events of Cenozoic time. It has resulted in ~2,000 km of north–south crustal shortening within continental Eurasia[1]. Several models have been proposed for the mechanism of this shortening: continuous deformation, multiple continental underthrusting, eastward propagating extrusion or mosaic tectonics[2–5]. Convergent plate motion still occurs between India and Eurasia and is evidenced in particular by active tectonics beneath the Himalayas, in Tibet and in south-central Asia[6–8].

The continental effects of the collision have been extensively studied, in particular during the 1980–83 French–Chinese cooperation programme in Tibet[5–9]. Geological or geophysical observations on land can only give bounds on the age of the initial collision. For instance, structural observations along the Yarlung Zangbo suture zone (YZSZ) in Tibet (in the vicinity of Lhasa) show the ophiolites to have been obducted before the end of the Eocene (before 40 Myr)[9]. Such a young upper bound is also indicated by petrological and geochronological data on igneous rocks in Tibet. Indeed, the youngest granodiorites observed near Lhasa are dated at 41 Myr (ref. 10) and thus may be consistent with the subduction of oceanic crust beneath Tibet until at least 45 Myr, assuming up to 4 Myr for the transit and cooling of magma in the crust. An older age for the initial collision has been proposed from geological evidence and seafloor spreading data[11]. It is suggested that it began, at least in the Ladakh area, before the middle Eocene (near 53 Myr).

On the other hand, only a few studies have analysed the consequences of the collision on plate tectonics. In an early analysis of seafloor spreading in the Indian ocean, Molnar and Tapponnier[12] interpreted a decrease in the rate of northward drift of India near 40 Myr as indicative of the India–Eurasia collision. Using more detailed data, this slowing of the Indian plate has been associated with the decrease in spreading rate on the Eastern Indian ridge near anomaly 22 time (~50 Myr)[13–15]. Following Molnar and Tapponnier[12], several authors have related this change in spreading rate to the collision between the two continental masses[16,17]. However, the change in India–Africa relative motion observed at anomaly 20 (44 Myr) has been considered elsewhere as indicative of this collision[17]. Also, evidence for an important plate reorganization in the north-eastern Indian Ocean after anomaly 20 time has recently been put forward and interpreted as a consequence of the collision[18].

Here we use a more comprehensive set of marine magnetic anomalies in the central Indian Ocean, in the vicinity of the triple junction[19] to determine the detailed motion of the Indian plate since anomaly 32 time (late Upper Cretaceous) and to clarify the chronology of the collision. The relative position of India with respect to Eurasia is computed using a procedure originally proposed by Patriat *et al.*[17]. It is then compared with its absolute position with respect to the hotspot frame of reference. This latter absolute motion is compared with recently determined palaeomagnetic poles in Ladakh, Tibet and Thailand[1,20–22] in order to determine the northern extent of India before the collision. The present data are combined with a recent interpretation of the northeastern Indian Ocean[18] to provide a complete reconstruction of the Indian plate before, and immediately after, the India–Eurasia continental collision. The relative importance of the driving forces of plate tectonics is then discussed taking into account these reconstructions.

Age of the India–Eurasia collision

In the past 15 yr, an extensive survey has been performed in the Indian Ocean using ships *Gallieni* and *Marion Dufresne* (see ref. 23). This survey has allowed a detailed interpretation of marine magnetic anomalies in the Central Indian Basin, the Crozet Basin and the Madagascar Basin[19,23] (Fig. 4*b*). These anomalies were generated at the accreting boundaries between the India, Antarctica and Africa plates, which meet at the Rodriguez triple junction. The simultaneous study of seafloor spreading on both flanks of these three ridges in the vicinity of the triple junction has allowed a complete and consistent